Inorganic Chemistry

Article

pubs.acs.org/IC

# Excited-State Interaction of Red and Green Perylene Diimides with Luminescent Ru(II) Polypyridine Complex

Rajeev K. Dubey,* Marja Niemi, Kimmo Kaunisto, Kati Stranius, Alexander Efimov, Nikolai V. Tkachenko, and Helge Lemmetyinen

Department of Chemistry and Bioengineering, Tampere University of Technology, P.O. Box 541, 33101 Tampere, Finland

Supporting Information

**ABSTRACT:** Three new perylene diimide (PDI)-based ligands have been synthesized by the covalent attachment of dipyrido[*a*,*c*]phenazine moiety to one of the bay-positions of PDI, while the second position has been substituted with either a 4-*tert*-butylphenoxy or a pyrrolidinyl group to obtain two types of chromophores, Ph-PDI and Py-PDI, respectively, with distinct properties. In the case of Py-PDI, the resultant 1,7- and 1,6-regioisomers have been successfully separated by column chromatography and characterized by $^{1}$H NMR spectroscopy. The ligands have been employed to prepare donor−acceptor-based ensembles incorporating the covalently linked PDI and Ru(II) polypyridine complex as the acting chromophores. A comprehensive study of the excited-state photodynamics of the ensembles has been performed by means of electrochemical and steady state and time-resolved spectroscopic methods. Although, in all the three ensembles, the photoexcitation of either chromophore resulted in a long-lived triplet excited state of PDI ($^{3}$PDI) as the final excited state, the photochemical reactions leading to the triplet states were found to be essentially different for the two types of the ensembles. In the case of the Ph-PDI-based ensemble, the excitation of either chromophore leads to the electron transfer from the Ru(II) complex to Ph-PDI, whereas for the Py-PDI-based ensembles, the electron transfer is observed in the opposite direction and only when the Ru(II) complex is excited. The difference in the behavior was rationalized based on electrochemical study of the compounds, which has shown that the Ph-PDI chromophore is a better electron acceptor and the Py-PDI chromophores are relatively better electron donors. This study shows a chemical approach to control the photoreactions in PDI-based dichromophoric ensembles including the possibility to switch the direction of the photoinduced electron transfer.

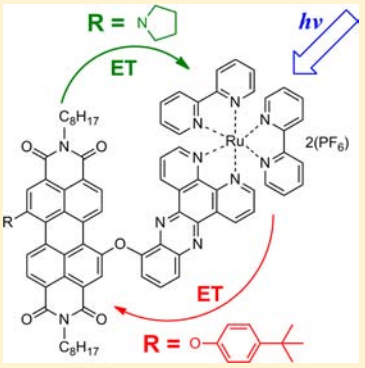


## INTRODUCTION

A better knowledge of the electronic interactions between photoactive components is highly essential not only to enhance our understanding of natural systems but also to develop new molecular photovoltaic, optoelectronic, and other photodriven applications.[1] During the past three decades, several photoactive units have been tested as integrative building blocks for the construction of donor−acceptor-based systems displaying various properties. Among these, the perylene diimide (PDI) dyes stand out as unique components because of their diverse and fascinating properties such as easy functionalization, excellent electron acceptor ability, high molar extinction coefficient in the visible region, high fluorescence quantum yields, and extraordinary photochemical stability.[2] In light of these properties, these dyes have been linked to various renowned organic and inorganic chromophores to construct useful systems for artificial photosynthesis, effective light-harvesting, and photochromism.[3] The possibility to fine-tune the optical and electrochemical properties of PDI further increases its use as a photofunctional material.

Inherently, PDIs have high electron affinity, and consequently, they are easy to reduce and rather difficult to oxidize. However, the presence of either electron-rich or electron-deficient substituents at the bay-region can modulate their redox and optical characteristics to a great extent.[2] For example, the substitution of strong electron-donating alkylamino substituents (Figure 1) makes the dye sufficiently electron-rich,

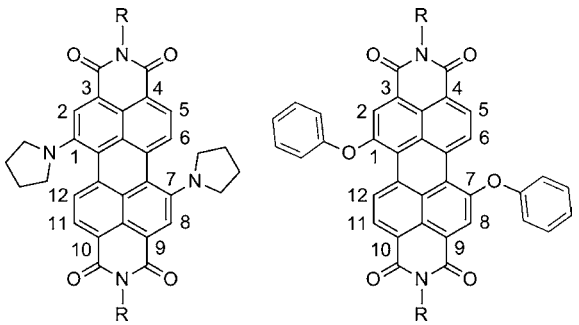

**Figure 1.** Chemical structures of green (left) and red (right) perylene diimides along with the numbering of the various positions of the PDI core.

so that the 1,7-derivatives exhibit even two oxidations at moderate potentials.[4] Simultaneously, the 1,7-derivatives (so-called green PDIs) display broad and strong absorption in the near IR

**Received:** February 22, 2013
**Published:** August 13, 2013





dx.doi.org/10.1021/ic400474b | *Inorg. Chem.* 2013, 52, 9761−9773

**Scheme 1. Synthesis of 1,7-Py- and 1,6-Py-PDI–Ru(II) Polypyridine Ensembles**[a]

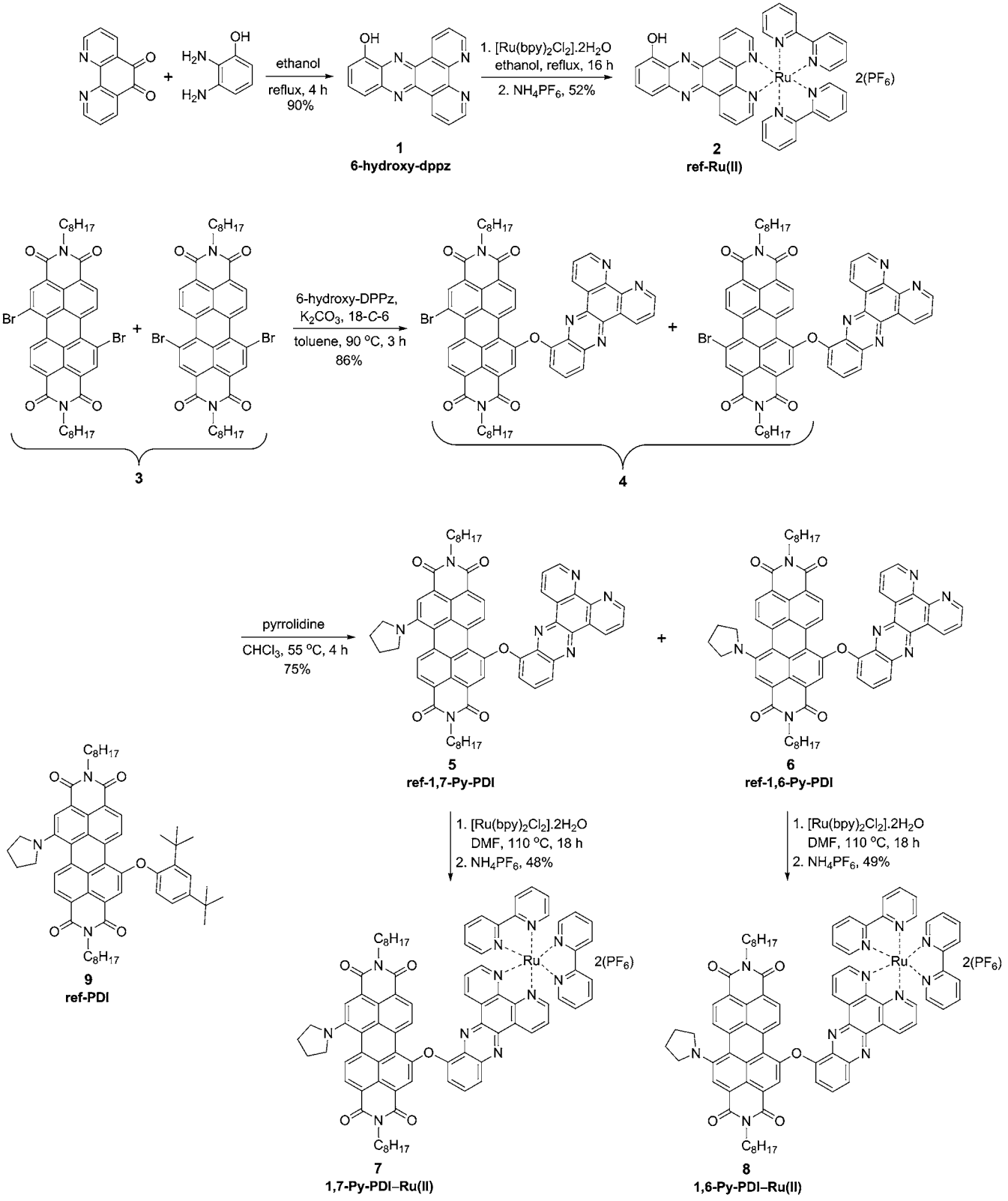


[a]Compounds **5** and **6** were utilized as reference PDIs in electrochemical and optical studies. Compound **9** (named as ref-PDI) was utilized for NMR analysis.

region, which helps to harvest solar energy efficiently. On the other hand, the phenoxy-substituted derivatives (so-called red PDIs, Figure 1) retain the basic optoelectronic properties and exhibit better solubility.[2]

A scrutiny of the previous research reveals that mostly PDIs with basic properties have been employed in systems incorporating the metal complexes. However, the excited-state behavior of the red PDI has been found to be different with


dx.doi.org/10.1021/ic400474b | Inorg. Chem. 2013, 52, 9761–9773

**Scheme 2. Synthesis of 1,7(6)-Ph-PDI–Ru(II) Polypyridine Dyad**[a]

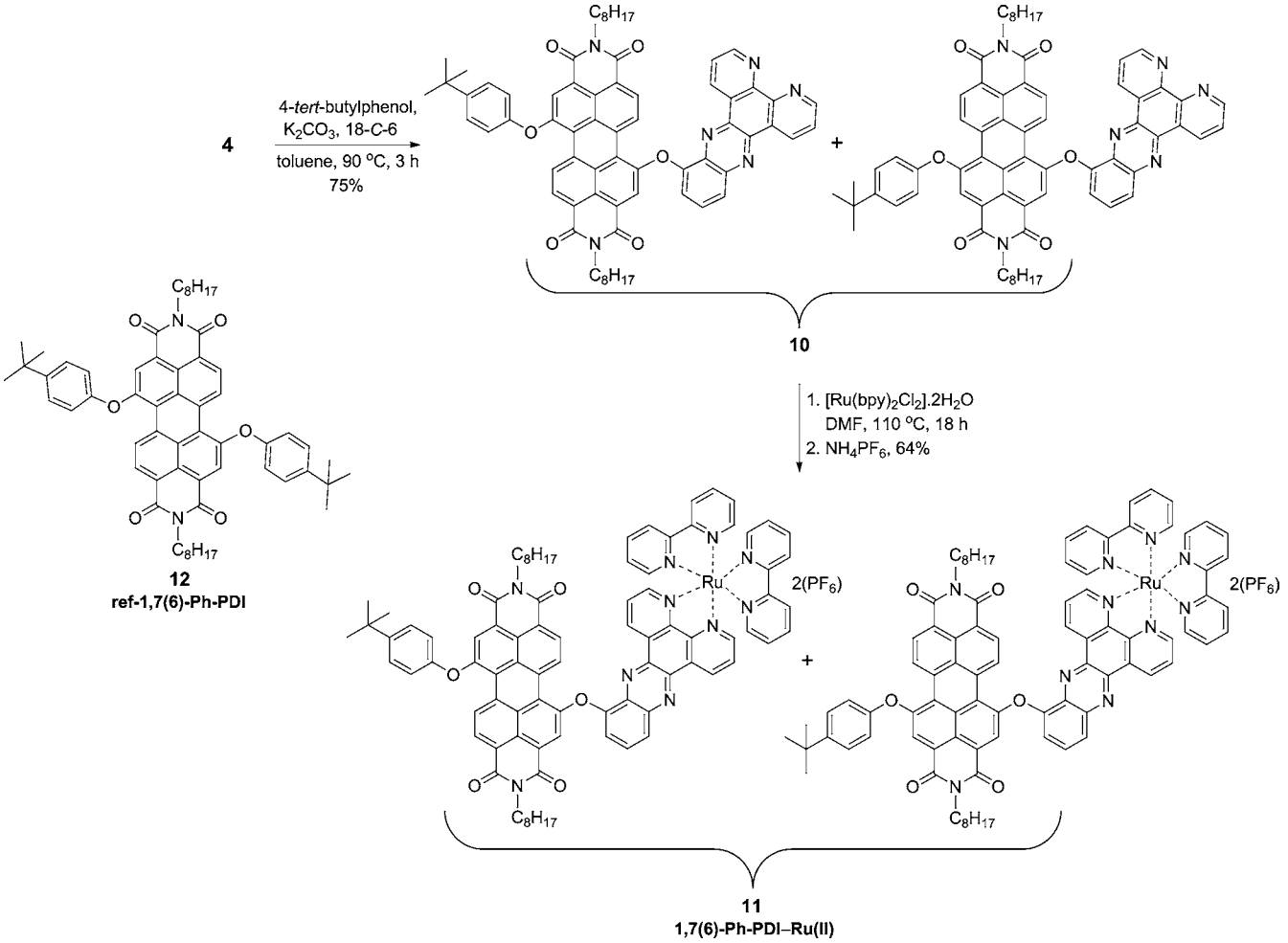


[a]Compound **12** was utilized as a reference PDI in the optical and electrochemical studies. It existed as a regioisomeric mixture (ref 9).

different metal systems. For example, in the recently reported Pt(II) square planar structures, with PDI covalently attached to the metal center through an acetylide linkage, the $^3$PDI excited state was successfully obtained as a result of strong spin–orbit coupling induced by Pt(II).[5] On the contrary, the strong fluorescence of the dye has been retained in the palladium complexes, despite the direct attachment of metal to the 1,7-bay-positions of PDI.[6] Similarly, other complexes of PDI–pyridine/terpyridine ligands with metals like Pt, Pd, Zn, Fe, and Ir possess a relatively high fluorescence quantum yield and a low yield of $^3$PDI excited state.[3g,7] Charge-transfer-based interactions have also been observed in the metal–organic hybrids, comprising red PDI and either Ru-porphyrin or Ru-phthalocyanine linked through axial coordination.[8] Interestingly, the excited-state dynamics of the two ensembles are different in spite of the similar design. In the phthalocyanine–PDI–phthalocyanine assembly, photoexcitation of either chromophore resulted in a long-lived charge-separated state with a lifetime of ≈115 ns. On the contrary, in the case of the porphyrin–PDI–porphyrin ensemble, an electron transfer from porphyrin to PDI ($\tau_{cs}$ = 5.6 and $\tau_{cr}$ = 270 ps) was observed only when PDI was excited, whereas photoexcitation of the porphyrin moieties resulted in a triplet energy transfer. Also in a recently reported PDI–[(bpy)Ru(II)Cl$_2$(CNbutyl)$_2$] system, charge transfer from the Ru complex to PDI was observed upon selective excitation of the PDI moiety.[3f] Thus, the PDI derivatives have been employed exclusively as electron acceptors in these charge-transfer-based metallo-organic assemblies.

Herein, we investigated the excited-state interaction of the covalently linked luminescent Ru(II) polypyridine complex with two different PDIs, namely, the red and green PDIs. To implement this idea, a dipyrido[*a*,*c*]phenazine (dppz) moiety was first covalently attached to one of the bay-positions of PDI. The dppz ligand was selected for this study mainly because of the synthetic ease by which a necessary active site can be generated on it. The second bay-position of the resultant PDI was subsequently substituted with either 4-*tert*-butylphenoxy or a pyrrolidinyl group to obtain electron-deficient and electron-rich PDI–dppz ligands, respectively. Finally, the obtained ligands were utilized to form the PDI–[Ru(bpy)$_2$(dppz)]$^{2+}$ ensembles. To the best of our knowledge, this is the first report in which the excited-state dynamics of the green PDIs have been investigated in the system comprising the transition metal. Interestingly, electron transfer was observed in all the PDI–Ru(II) polypyridine ensembles (i.e., with both the green and red PDIs). However, the direction of electron transfer (ET) was the opposite; when attached to the Ru(II) complex, the green PDIs acted as electron donors and the red PDI as an acceptor.


dx.doi.org/10.1021/ic400474b | Inorg. Chem. 2013, 52, 9761–9773

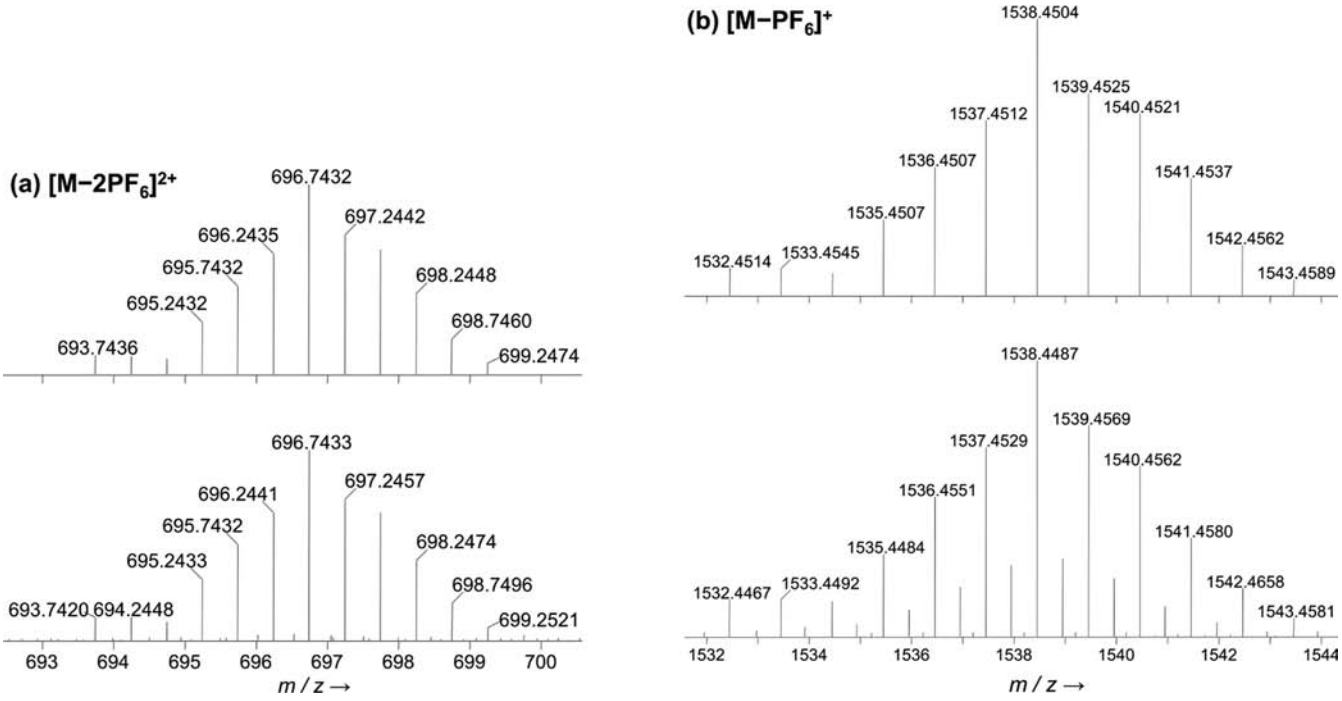


**Figure 2.** Comparison of the calculated (top) and the measured (bottom) spectra of the species (a) $[M - 2PF_6]^{2+}$ and (b) $[M - PF_6]^{+}$ of the ensemble 1,7-Py-PDI−Ru(II) **7**.

## RESULTS AND DISCUSSION

**Synthesis and Characterization.** All three perylene diimide−Ru(II) polypyridine ensembles (namely, 1,7-Py-PDI−Ru(II) **7**, 1,6-Py-PDI−Ru(II) **8**, and 1,7(6)-Ph-PDI−Ru(II) **11**) were synthesized from dibromo-PDI **3** according to the route summarized in Schemes 1 and 2.[9] In the very first step, 1,10-phenanthroline-5,6-dione and 2,3-diaminophenol were condensed in refluxing ethanol to obtain 6-hydroxy-dipyrido[*a*,*c*]phenazine (dppz) **1** in 90% yield. Subsequently, *N*,*N*′-dioctyl-1-bromo-7(6)-(dipyridophenazinoxy)perylene diimide **4** was prepared in 86% yield by the reaction of dppz **1** with dibromo-PDI **3**, which was a regioisomeric mixture. The analysis of the $^1$H NMR spectrum (300 MHz, $CDCl_3$) of the product **4** revealed the presence of 1,7- and 1,6-derivatives in a ratio of ≈60:40. The two isomers could not be separated by column chromatography in spite of the presence of the bulky dppz moiety at the bay-region. Consequently, the regioisomeric mixture **4** was used for the next step in which the free bromine atom of the compound **4** was substituted by either the pyrrolidine or the 4-*tert*-butylphenoxy group.

The attachment of the pyrrolidine group to the PDI bay-region is usually carried out by heating dibromo-PDI in neat pyrrolidine.[10] In our case, however, compound **4** was very poorly soluble, and the reaction did not yield any product under these conditions. To resolve this problem, compound **4** was first dissolved in $CHCl_3$, and subsequently, pyrrolidine was added to the reaction mixture in excess. The resulting deep-red solution of **4** in the $CHCl_3$−pyrrolidine mixture was stirred at 55 °C for 4 h. The reaction progressed smoothly, as evidenced by TLC, to afford a regioisomeric mixture of the desired green ligands (**5** + **6**). The product was purified by column chromatography (silica 100, $CHCl_3$) and characterized by $^1$H NMR spectroscopy and mass spectrometry. In the NMR spectrum, the characteristic doublets and singlets of the PDI bay-protons corresponding to the 1,7- and 1,6-isomers were well-resolved. The integration areas of these signals revealed that the 1,7- and 1,6-derivatives (**5** and **6**) were present in a ratio of ≈68:32.

According to previous reports, the 1,7- and 1,6-regioisomers of PDI exhibit different redox and optical properties when strong electron-donating groups (e.g., pyrrolidine) are attached at the bay-positions.[9,11] In view of these results, we have separated the resultant 1,7- and 1,6-regioisomers (**5** and **6**) by column chromatography (silica 100, $CHCl_3$/toluene 1:1). In order to achieve complete separation, the purification process had to be repeated several times with slow elution due to the very similar retentions of the two isomers on silica. The separation of these isomers was confirmed by $^1$H NMR spectroscopy. The attachment of the pyrrolidinyl group at the bay-position changed the color of the ligands from red to deep green. In addition, the presence of the pyrrolidinyl group increased the solubility of the resulting ligands in polar solvents (specifically in DMF) tremendously, which was essential as the complexation reaction with $[Ru(bpy)_2Cl_2]\cdot 2H_2O$ is possible only in polar solvents, owing to the poor solubility of $Ru(bpy)_2Cl_2$ in moderately polar solvents.

In the final step, the PDI−Ru(II) polypyridine ensembles (**7** and **8**) were prepared by heating the solutions of the corresponding ligands in DMF with 2 equiv of $[Ru(bpy)_2Cl_2]\cdot 2H_2O$. The resulting Ru(II) polypyridine complexes were purified by column chromatography (alumina, $CHCl_3$−EtOH). Subsequently, chloride counteranions were exchanged with hexafluorophosphate anions by the addition of an excess of an aqueous solution of $NH_4PF_6$ to the ethanolic solution of the complex to obtain final products (**7** and **8**) in ≈50% yield. This exchange of counteranions from $Cl^-$ to $PF_6^-$ allowed the isolation of ensembles by precipitation.

The ref-Ru(II) complex **2** was synthesized by the reaction between 6-hydroxy-dipyrido[*a*,*c*]phenazine **1** and $[Ru(bpy)_2Cl_2]\cdot 2H_2O$ in ethanol, as depicted in Scheme 1. The synthesis of compound **9** (named as ref-PDI) was carried out


dx.doi.org/10.1021/ic400474b | *Inorg. Chem.* 2013, 52, 9761−9773

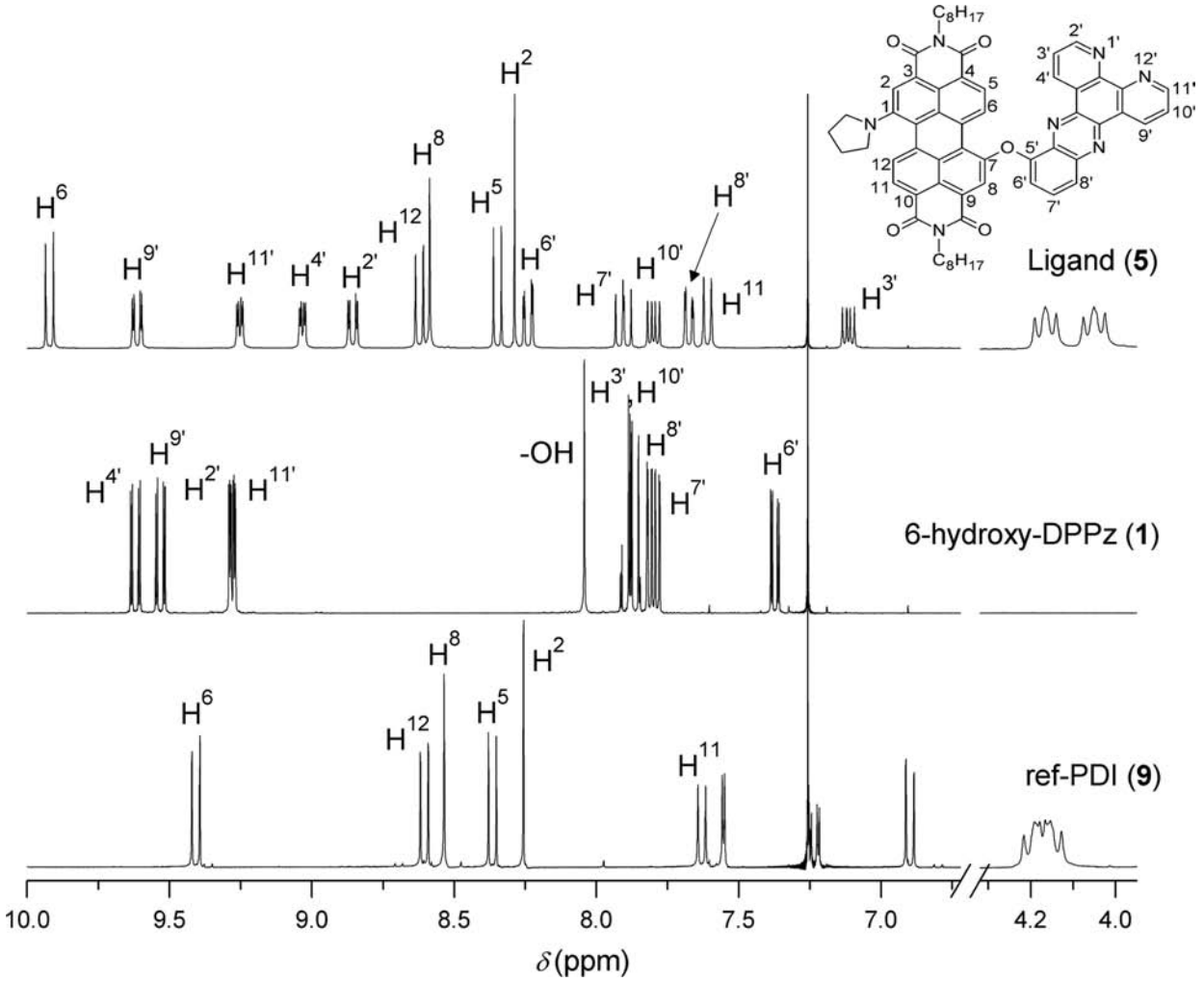


**Figure 3.** $^1$H NMR spectra of ligand (**5**), 6-hydroxy-DPPz (**1**), and ref-PDI (**9**).

from dibromo-PDI **3** by the sequential substitution of the two bromine atoms by 2,4-di-*tert*-butylphenoxy and pyrrolidinyl groups. The 1,7-isomer was successfully isolated in the pure form by column chromatography on silica 100 using toluene as eluent. Compound **9** was utilized as a reference in the $^1$H NMR analysis of ligand **5** (discussed separately in the next section).

The synthesis of the third ensemble, namely, 1,7(6)-Ph-PDI−Ru(II) polypyridine **11**, was carried out as summarized in Scheme 2. First, the 4-*tert*-butylphenoxy group was attached to compound **4**. In this case, keeping in mind the very similar properties of 1,7- and 1,6-regioisomers of phenoxy-substituted PDI, the resultant regioisomeric mixture **10** was used as such for the preparation of final compound **11** following the aforementioned procedure.

All the synthesized compounds, except the ensembles **7**, **8**, and **11**, were characterized by $^1$H NMR spectroscopy and mass spectrometry. For the ensembles, the $^1$H NMR spectra were not conclusive because of the strong aggregation and excessive broadening of the peaks. However, the high-resolution ESI-MS confirmed the formation of the ensembles. In the spectrum, the experimental masses and the isotopic patterns of the species, (a) $[M - 2PF_6]^{2+}$ and (b) $[M - PF_6]^{+}$, closely matched with the calculated ones with an accuracy of 1.0 and 2.3 ppm, respectively. Moreover, the isotopic distributions of these species were found in very good agreement with the calculated isotopic patterns, as shown in Figure 2.

**$^1$H NMR Analysis of Ligand 5.** A comparison of the $^1$H NMR spectrum of ligand **5** with the spectra of the corresponding reference compounds, 6-hydroxy-dppz **1** and ref-PDI **9** (the structures are shown in Scheme 1), provided some knowledge about the mutual orientation of the PDI and dppz moieties in the synthesized ligands (Figure 3). The assignment of the protons was made with the help of $^1$H−$^1$H COSY measurements (Figure S1, Supporting Information). The $^1$H NMR spectrum of the ligand displayed some characteristic features, indicating that the dppz moiety is oriented toward the PDI core. In the ligand, the close proximity of the two moieties resulted in a systematic shift to the signals of nearly all the protons of the dppz fragment. Thus, the protons $H^{2'}$, $H^{3'}$, and $H^{4'}$ are largely shifted upfield. This indicates that these protons are closer to the perylene core and are shielded by the PDI $\pi$-electrons. On the other hand, only small shifts were observed for the other group of protons, namely, $H^{9'}$, $H^{10'}$, and $H^{11'}$, which indicates that these protons are located away from the perylene core. Two protons, $H^{6'}$ and $H^{7'}$, experienced the deshielding effect and largely shifted downfield. Similarly, the effect of the dppz $\pi$-electrons is also observed on the PDI protons. The bay-proton, namely, $H^6$, is the one which is affected most and hence exhibited a downfield shift of 0.52 ppm.

**Steady State Absorption Studies.** The absorption spectra of the PDI−Ru(II) polypyridine ensembles in acetonitrile


dx.doi.org/10.1021/ic400474b | *Inorg. Chem.* 2013, 52, 9761−9773

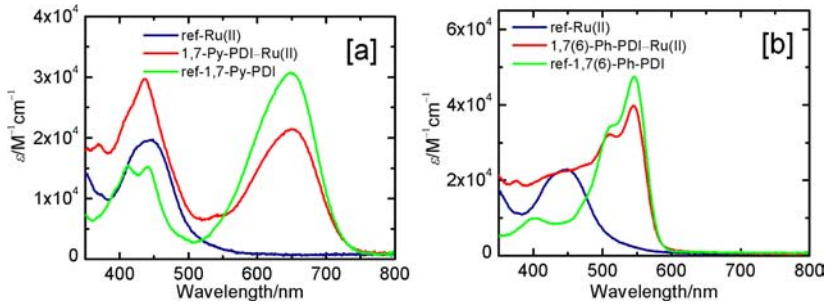


**Figure 4.** Steady state absorption spectra of ensembles (a) 1,7-Py-PDI–Ru(II) and (b) 1,7(6)-Ph-PDI–Ru(II) and their corresponding reference compounds in acetonitrile.

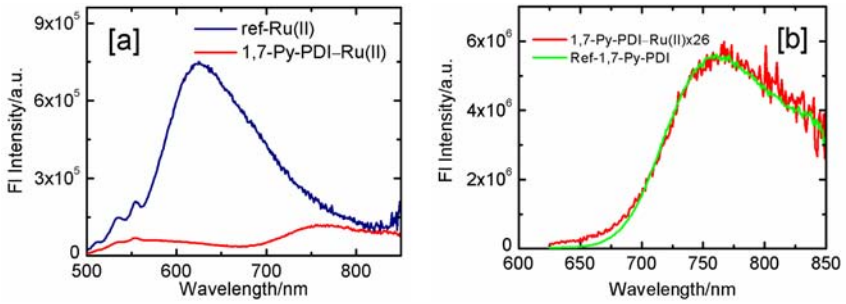


**Figure 5.** Comparison of the steady state emission spectra of the 1,7-Py-PDI–Ru(II) ensemble: (a) with ref-Ru(II), $\lambda_{ex}$ = 470 nm; (b) with ref-1,7-Py-PDI, $\lambda_{ex}$ = 605 nm. The spectrum of the ensemble has been multiplied by 26 for comparison in panel [b].

are shown in Figure 4, together with the corresponding reference compounds.

The absorption of the Ru(II) chromophore is dominated by its characteristic $^1$MLCT transition centered at ≈438 nm. The complex has very low absorption at wavelengths longer than 500 nm. On the other hand, the spectrum of the PDI chromophore is characterized by an intense band attributed to the $S_0$–$S_1$ electronic transition. In the case of the pyrrolidine-substituted PDIs (ref-1,7-Py-PDI and ref-1,6-Py-PDI), the lowest energy band is located between 550 and 750 nm with a maximum at 650 nm. The chromophores also exhibit a higher energy transition ($S_0$–$S_2$) band around 430 nm (Figure 4a). For the phenoxy-substituted PDI (red PDI), the absorption band is located between 450 and 590 nm with the maximum at ≈545 nm (Figure 4b).

The PDI–Ru(II) polypyridine ensembles exhibited characteristic absorption features of both the moieties. At shorter wavelengths, the absorption is dominated by a MLCT transition originating from the Ru(II) complex, whereas the absorption at wavelengths longer than 500 nm originates exclusively from the PDI chromophore. Therefore, it is possible to selectively excite the PDI chromophore. In contrast, the selective excitation of the Ru(II) chromophore is difficult due to the overlapping of its MLCT transition with the $S_0$–$S_2$ transition of the PDI.

**Steady State Emission Studies.** The two acting chromophores of the ensembles exhibit very different emission characteristics. The Ru(II) polypyridine complex has a broad emission between 550 and 850 nm with the maximum around 625 nm (Figure 5a). The emission originates from the $^3$MLCT state ($\Phi_{ph}$ = ∼0.02, $\tau_{ph}$ = ∼850 ns in deoxygenated acetonitrile) and is highly sensitive to the presence of oxygen.[12] On the other hand, the PDI chromophore displays a stronger emission, which originates from its singlet excited state ($S_1$). In the case of the pyrrolidine-substituted PDIs, ref-1,7-Py-PDI and ref-1,6-Py-PDI, the emission is located between 700 and 850 nm ($\lambda_{max}$ ≈ 750 nm, Figure 5b). These green PDIs have a fluorescence quantum yield of ≈0.08 in acetonitrile (Table 1).

**Table 1. Fluorescence (fl) Quenching of the PDI Moiety in PDI–Ru(II) Ensembles in Acetonitrile**

| compound | fl quenching[a] | $\Phi_{fl}$[d] |
|---|---|---|
| 1,7-Py-PDI–Ru(II) | 97%[b], 96%[c] | 3.3 × 10$^{-3}$ (0.08) |
| 1,6-Py-PDI–Ru(II) | 91%[b], 89%[c] | 3.9 × 10$^{-3}$ (0.07) |
| 1,7(6)-Ph-PDI–Ru(II) | 98%[b], 97%[c] | 2.0 × 10$^{-2}$ (0.83) |

[a]Fluorescence quenching of the PDI moiety. [b]When the Ru(II) chromophore was predominantly excited. [c]When the PDI moiety was selectively excited. [d]Fluorescence quantum yield of the PDI moiety ($\Phi_{fl}$ values of the corresponding ref-PDIs are given in the parentheses).

The phenoxy-substituted PDI displays an extremely strong emission ($\Phi_{fl}$ = 0.83), which is located between 550 and 750 nm with the maximum around 580 nm in acetonitrile (Figure S2, Supporting Information).

To study the effect of the Ru(II) polypyridine chromophore on the PDI moiety, the ensembles and reference compounds were excited at two separate wavelengths. The selective excitation of the PDI moiety was achieved using an excitation wavelength longer than 510 nm. The blue excitation (445 nm for the 1,7(6)-Ph-PDI–Ru(II) ensembles; 470 nm for the 1,7-Py-PDI–Ru(II) and the 1,6-Py-PDI–Ru(II) ensembles) was used to probe the effect of the excited Ru(II) chromophore; at the selected wavelengths, roughly two-thirds of the primary excited chromophores are the Ru(II) chromophores of the ensembles. In all the ensembles, the emission of the PDI moieties was found to be significantly quenched independent of the excitation wavelength (Table 1). For example, in the ensemble 1,7(6)-Ph-PDI–Ru(II), the emission of the PDI


dx.doi.org/10.1021/ic400474b | Inorg. Chem. 2013, 52, 9761–9773

Table 2. Redox Potentials (V vs. Ag/AgCl) of Ensembles and Reference Compounds Obtained by DPV[a]

| compound | $E_{1ox}$ | $E_{2ox}$ | $E_{1red}$ | $E_{2red}$ | $E_{3red}$ | $E_{S1}$[c] (eV) | $E_{3MLCT}$[d] | $E_{CS}$[e] (eV) |
|---|---|---|---|---|---|---|---|---|
| ref-Ru(II) | +1.37 | | −0.90 | −1.30 | −1.46 | | 2.1 | |
| ref-1,7-Py-PDI | +0.90 | +1.33 | −0.73 | −0.93 | | 1.8 | | |
| 1,7-Py-PDI−Ru(II) | +0.90 | +1.38[b] | −0.67 | −0.87 | −0.99 | 1.8 | | 1.77 {PDI$^{\bullet+}$−Ru(II)$^{\bullet-}$} |
| ref-1,6-Py-PDI | +0.95 | +1.47 | −0.70 | −0.88 | | 2.2 | | |
| 1,6-Py-PDI−Ru(II) | +0.94 | +1.40[b] | −0.67 | −0.87 | −1.00 | | | 1.81 {PDI$^{\bullet+}$−Ru(II)$^{\bullet-}$} |
| ref-1,7(6)-Ph-PDI | +1.43 | +1.72 | −0.61 | −0.84 | | | | |
| 1,7(6)-Ph-PDI−Ru(II) | +1.42[b] | +1.70 | −0.55 | −0.80 | −0.97 | | | 1.97 {PDI$^{\bullet-}$−Ru(III)} |

[a]Scan rate: 0.05 V/s. [b]Peaks of the PDI and Ru(II) chromophores are merged. [c]Energy of the singlet excited state of PDI. [d]Energy of the 3MLCT state of the Ru(II) complex calculated from absorption and emission measurements. [e]Energy of the lowest charge-separated state; $[E_{CS} = E_{1ox}(D) - E_{1red}(A)]$.

moiety was quenched at 98% ($\Phi_{fl}$ = 0.02) in comparison to that of ref-PDI ($\Phi_{fl}$ = 0.83). Similarly, the emission of the Ru(II) chromophore was also found to be quenched when the Ru(II) chromophore of the ensembles was predominantly excited (Figure 5a). However, the accurate value of the quenching could not be determined due to overlapping of the emission bands of the two chromophores.

The emission studies revealed the quenching of the singlet excited state of the PDI moiety by the appended Ru(II) chromophore. This observation demonstrates that an efficient nonradiative deactivation of $^1$PDI* dominates upon metal coordination. The possible mechanisms for the quenching may be either an electron or an energy transfer between the two moieties or an efficient intersystem crossing due to the heavy atom effect exerted by the Ru metal. The possibility of the electron transfer reactions can be evaluated on the basis of the redox properties of the compounds.

**Electrochemistry.** The electrochemical properties of all the ensembles and the individual entities were examined by differential pulse voltammetry. The measurements were carried out in benzonitrile containing 0.1 M tetrabutylammonium tetrafluoroborate as supporting electrolyte. The obtained redox potentials (V vs Ag/AgCl) are summarized in Table 2, and the voltammograms are shown in Figure S3 (Supporting Information). The energies of the charge-separated states for the ensembles were estimated by the difference between the first oxidation potential of the donor and the first reduction potential of the acceptor $[E_{CS} = E_{1ox}(D) - E_{1red}(A)]$. In this estimation, the electrostatic interactions and solvent dielectric effects were excluded mainly because it was rather difficult to say which model should be used to estimate the Coulombic interaction. Often the donor and acceptor are considered as spherical, and the Rehm−Weller equation is used to estimate the energy of the charge-separated state. However, the moieties are not really spheres in this case, and thus, the Rehm−Weller equation may provide a quite inaccurate estimation. Furthermore, the effect of this particular solvent (acetonitrile) is expected to be rather small because it is highly polar ($\varepsilon$ = 37.5).

The reference Ru(II) polypyridine complex (**2**) exhibits a reversible one-electron oxidation at +1.37 V, which is assigned to the Ru(II)/Ru(III) redox couple. The complex exhibits three ligand-based one-electron reductions at high potentials (−0.90, −1.30, and −1.46 V) assigned to the reductions of the dppz and the bipyridine ligands.[12,13] The phenoxy-substituted PDI, ref-1,7(6)-Ph-PDI, exhibited a typical voltammogram of red PDI with two reductions at low potentials (−0.61 and −0.84 V) and two oxidations at high potentials (+1.43 and +1.72 V). On the other hand, the pyrrolidinyl-functionalized PDIs, ref-1,7-Py-PDI and ref-1,6-Py-PDI, exhibited relatively higher values for the first reduction potentials (−0.73 and −0.70 V, respectively) and significantly lower values of the first oxidation (+0.90 and +0.95 V, respectively). These observations demonstrate that Ph-PDI is a good electron acceptor and that the Py-PDIs are reasonably good electron donors. There are relatively small perturbations of redox potentials of the chromophores in the ensemble structures, and the lowest energy charge-separated states can be predicted as PDI$^{\bullet+}$−Ru(II)$^{\bullet-}$ for 1,7-Py-PDI−Ru(II) and 1,6-Py-PDI−Ru(II) with the energies of 1.77 and 1.81 eV, respectively, and PDI$^{\bullet-}$−Ru(III) for 1,7(6)-Ph-PDI−Ru(II) with an energy of 1.97 eV relative to the energies of the ground states. It is important to notice that the direction of the charge transfer in the third ensemble is opposite to that of the first two.

The energies of the excited states were evaluated on the basis of the absorption and emission measurements and are presented in Table 2. Comparing the energies of the charge-separated states and the energies of the excited states, one can conclude that for the 1,7-Py-PDI−Ru(II) and 1,6-Py-PDI−Ru(II) ensembles the only energetically favorable ET process is from the triplet excited MLCT state, that is, PDI−$^{3MLCT}$Ru(II)* → PDI$^{\bullet+}$−Ru(II)$^{\bullet-}$. For the ensemble 1,7(6)-Ph-PDI−Ru(II), however, either excited chromophore may undergo the charge transfer, PDI−$^{3MLCT}$Ru(II)* → PDI$^{\bullet-}$−Ru(III) and $^1$PDI*−Ru(II) → PDI$^{\bullet-}$−Ru(III).

**Transient Absorption Studies.** The excited-state dynamics of all the ensembles were studied on both nanosecond and picosecond time scales with flash photolysis and pump−probe methods, respectively. In the flash-photolysis measurements, the acetonitrile solutions of the ensembles and reference compounds were excited at 420 nm, where both PDI and the Ru complex absorb almost equally, and at 532 nm, where PDI absorbs exclusively. Also, the pump−probe measurements were carried out with 420 nm excitation for all compounds. In addition, for the 1,7-Py-PDI−Ru(II) dyad, the pump−probe measurements were done with excitation at 600 nm, where only the PDI chromophore absorbs.

In the flash-photolysis measurements, the transient absorption decays of all dyad samples were found to be monoexponential at all the monitoring wavelengths. The long-lived triplet state of PDI was detected as the only intermediate state by its characteristic absorptions in the ranges of 400−500 and 575−800 nm or 450−550 and 700−900 nm for the Ph-PDI ensemble and the Py-PDI ensembles, respectively.[14] In addition, a bleaching of the ground-state absorption band of PDI was observed with minima for Ph-PDI and Py-PDI at 540 and 650 nm, respectively. The triplet character of this species was also confirmed by its quenching with molecular oxygen.


dx.doi.org/10.1021/ic400474b | Inorg. Chem. 2013, 52, 9761−9773

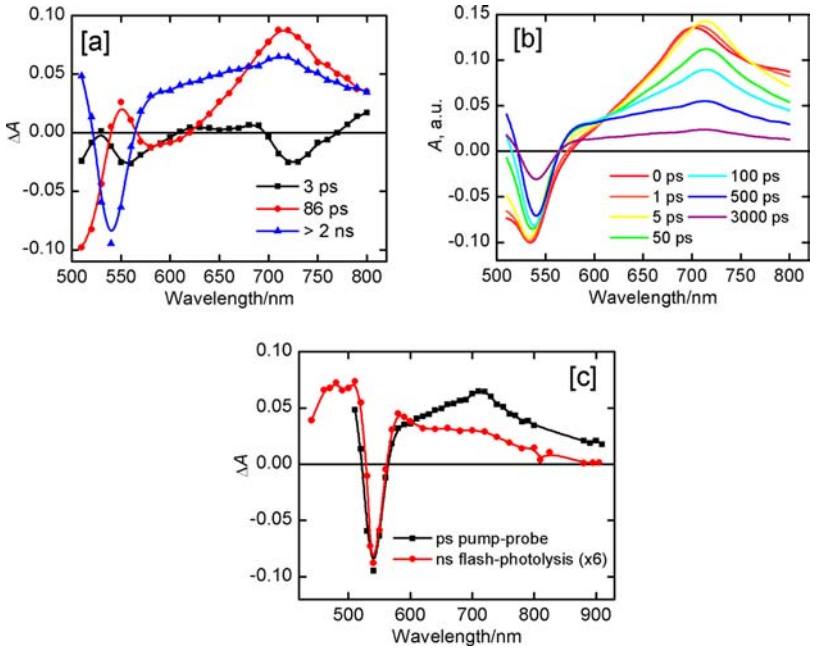


**Figure 6.** (a) Picosecond transient absorption decay component spectra of the ensemble 1,7(6)-Ph-PDI–Ru(II) obtained after the laser excitation at 420 nm in acetonitrile. (b) Time-resolved spectra calculated at selected delay times. (c) Comparison of the longest-lived spectrum obtained in the picosecond pump–probe measurement and the spectrum from the nanosecond flash-photolysis measurement.

The transient absorption decay curves at different wavelengths, obtained from the pump–probe measurements, were fitted globally to identify the intermediate states and time constants of the reaction steps. The measurements of ref-Ru(II) (Figure S4, Supporting Information) indicated a fast increase in absorption around 600–700 nm, 1.8 ps, which can be attributed to an intraligand electron transfer (ILET).[15] The 420 nm excitation promotes the Ru complex to its $^{1}$MLCT state, and extremely rapid intersystem crossing (<100 fs) yields $^{3}$MLCT$^{prox}$ as the first state observed within the time resolution of our instrument (spectrum at 0 ps, Figure S4, Supporting Information). In the $^{3}$MLCT$^{prox}$ state, the electron is localized on the bipyridine part of the dppz ligand. Subsequently, it is transferred to the phenazine part by the ILET process, yielding the energetically lower $^{3}$MLCT$^{dis}$ state.[16] The characteristic features of the first singlet excited state of ref-1,7(6)-Ph-PDI, $^{1}$Ph-PDI*, are a band at around 700 nm and a bleaching of the ground-state absorption (i.e., a negative band at 540 nm) (Figure S4, Supporting Information).

The decay component spectra of the ensemble 1,7(6)-Ph-PDI–Ru(II) are presented in Figure 6a. The time-resolved absorption right after the excitation (at 0 ps) shows typical features of the first singlet excited state of the PDI chromophore. Even though the Ru(II) chromophore of the ensemble is equally excited at 420 nm, its excited state is not well-observed at this time because it is less intense and does not provide characteristic features. The first resolved process (3 ps) results in a rise of the absorption at 710 nm and minor changes in the region of the PDI ground-state absorption. The following process (86 ps) raises the bleaching of the PDI ground-state absorption and reshapes the absorption in the red part of the spectrum. The longest-lived spectrum detected in the pump–probe measurements shows a gradual bleaching of the PDI ground-state absorption at 540 nm and a new absorption band at 710 nm. The band at 710 nm was previously attributed to the PDI anion, and this state can be recognized as the charge-separated state, PDI$^{\bullet-}$–Ru(III), with an electron transferred from Ru to PDI.[3f,8b,17]

The two-step formation of this state can be rationalized considering that two different chromophores were excited by the laser flash at 420 nm. We tend to conclude that the faster CS (3 ps) takes place starting from the PDI excited singlet state, $^{1}$PDI*–Ru(II) → PDI$^{\bullet-}$–Ru(III), and the slower CS (86 ps) from the triplet excited state of the Ru complex, PDI–$^{3MLCT(dis)}$Ru(II)* → PDI$^{\bullet-}$–Ru(III), because the slower process increases the PDI ground-state bleaching, and thus, its initial state should have the PDI chromophore in its ground state. This also agrees with the higher driving force of the electron transfer starting from the singlet excited state $^{1}$PDI*–Ru(II) as compared to that from the triplet state PDI–$^{3MLCT(dis)}$Ru(II)* in the Marcus normal regime of the electron transfer. In this experiment, the ILET process, PDI–$^{3MLCT(prox)}$Ru(II)* → PDI–$^{3MLCT(dis)}$Ru(II)*, was not resolved because it overlaps in time with the faster step of CS from the excited PDI, and the overall spectral changes associated with the ILET reaction are weaker than those of the PDI to Ru(II) CT reaction.

The formed CS state has a relatively long lifetime, and its decay was not seen in the pump–probe experiments, where the maximum delay time is 1.4 ns. The time resolution of the flash-photolysis instrument that was used is limited to 100 ns, and the spectrum obtained at this delay time differs from the final spectrum detected in the pump–probe experiments (Figure 6c). In both cases, the sharp negative peak at 540 nm indicates that the PDI chromophore is not in its ground state. The difference in the red part shows that at 100 ns the PDI chromophore is in the triplet state, whereas at ∼1 ns the ensemble is in the CS state. Thus, the charge recombination, PDI$^{\bullet-}$–Ru(III) → $^{3}$PDI*–Ru(II), takes place in the time interval between 1 and 100 ns. The exact value, however, cannot be determined with the instruments that were used for this study.


dx.doi.org/10.1021/ic400474b | Inorg. Chem. 2013, 52, 9761–9773

The proposed reaction scheme for the ensemble 1,7(6)-Ph-PDI–Ru(II) is summarized in Figure 7. The fast internal

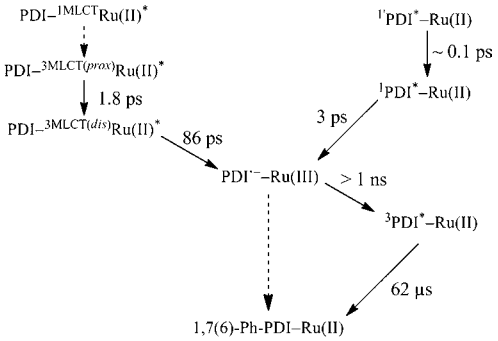


**Figure 7.** Proposed reaction scheme depicting the photophysical processes occurring in the ensemble 1,7(6)-Ph-PDI–Ru(II). The dashed arrows represent probable processes, which were not resolved with the instruments that were used in this study.

conversion of the second singlet excited state of PDI, $^{1'}$PDI*–Ru(II), is shown tentatively as it was not time-resolved. Similarly, ILET in the Ru complex was observed only for the reference compound but not for the ensemble. However, it is reasonable to assume that this fast process will remain fast in the ensemble. Other time constants that are shown in Figure 7 were obtained from the pump–probe and flash-photolysis measurements.

The decay component spectra of 1,7-Py-PDI–Ru(II) are shown in Figure 8. Essentially, the same spectra and very similar lifetimes were obtained for 1,6-Py-PDI–Ru(II) (Figure S6, Supporting Information). Similar to the 1,7(6)-Ph-PDI–Ru(II) ensemble, the intersystem crossing and ILET of the Ru complex were not resolved for 1,7-Py-PDI–Ru(II). For 1,6-Py-PDI–Ru(II) (Figure S6, Supporting Information), a rather featureless fast process (0.4 ps) was resolved. This can be attributed to a combination of ILET in the Ru(II) complex and internal conversion in PDI. The first time-resolved process in 1,7-Py-PDI–Ru(II), 3 ps, shows a gradual increase in the bleaching of the ground-state absorption of the PDI chromophore. The process can be either an energy transfer or an electron transfer. Considering that the 3 ps component shows also some increase in the absorption at ≈750 and 550 nm, we assume that the reaction is the charge transfer, PDI–$^{3MLCT(dis)}$Ru(II)* → PDI$^{\bullet+}$–Ru(II)$^{\bullet-}$.[4]

In 53 ps, the triplet state of the PDI chromophore is formed, which then decays in a microsecond time domain as revealed by the flash-photolysis experiments (Figure 8c). In contrast to the case of 1,7(6)-Ph-PDI–Ru(II), the final transient seen in the pump–probe measurement is the same as the transient obtained in the flash-photolysis measurement (Figure 8c); that is, the formation of the PDI triplet was resolved in pump–probe and the decay in the flash-photolysis measurement. The triplet state can be formed by two reactions: firstly by the charge recombination, PDI$^{\bullet+}$–Ru(II)$^{\bullet-}$ → $^{3}$PDI*–Ru(II), and secondly by the intersystem crossing of the PDI chromophore, $^{1}$PDI*–Ru(II) → $^{3}$PDI*–Ru(II). Since the singlet excited state, $^{1}$PDI*–Ru(II), is also generated by the excitation at 420 nm, and the intersystem crossing was not observed for the reference PDIs in this time scale, we have to conclude that the intersystem crossing of the PDI chromophore is strongly facilitated by the presence of Ru in the ensemble. Essentially, the same results were obtained with excitation at 600 nm for 1,7-Py-PDI–Ru(II) except that ET was not observed, and only the intersystem crossing was seen with a time constant of 36 ps (Figure S7, Supporting Information).

The reaction scheme for the ensembles 1,6-Py-PDI–Ru(II) and 1,7-Py-PDI–Ru(II) is the same, and it is presented in Figure 9 with time constants indicated for 1,7-Py-PDI–Ru(II). The time constant (0.4 ps) for the internal conversion of the

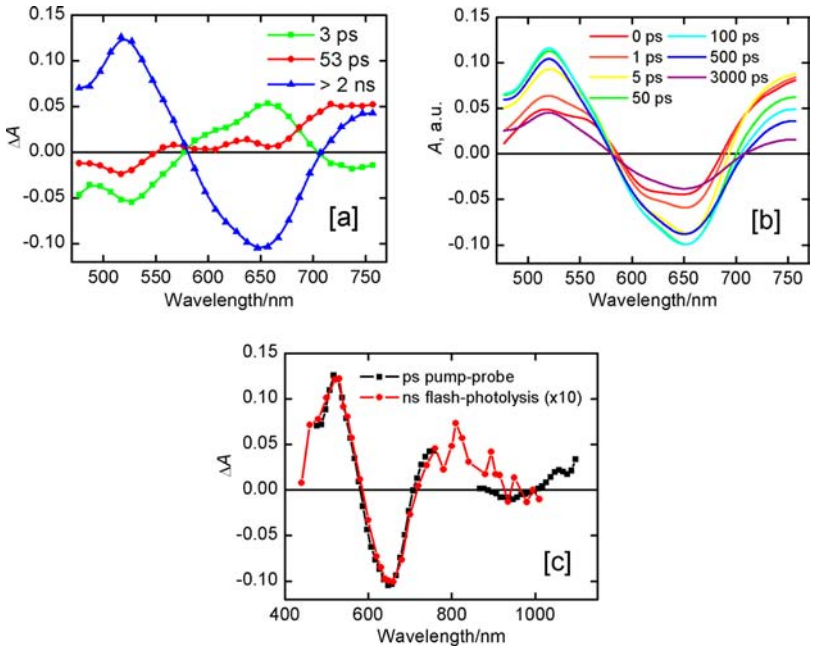


**Figure 8.** (a) Picosecond transient absorption decay component spectra of the ensemble 1,7-Py-PDI–Ru(II) obtained after the laser excitation at 420 nm in acetonitrile. (b) Time-resolved spectra calculated at selected delay times. (c) Comparison of the longest-lived spectrum obtained in the picosecond pump–probe measurement and the spectrum from the nanosecond flash-photolysis measurement.


dx.doi.org/10.1021/ic400474b | Inorg. Chem. 2013, 52, 9761–9773

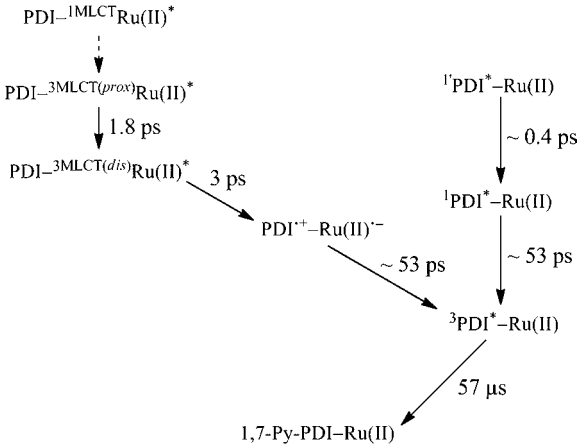


**Figure 9.** Proposed reaction scheme for the ensembles 1,7-Py-PDI–Ru(II) and 1,6-Py-PDI–Ru(II) with time constants mentioned for 1,7-Py-PDI–Ru(II).

second excited state of the PDI chromophore is taken from the measurement of the ensemble 1,6-Py-PDI–Ru(II). However, the time constant (1.8 ps) for the ILET of the Ru(II) complex is taken from the measurement of corresponding reference compound.

The essential difference between 1,7(6)-Ph-PDI–Ru(II) and the other two ensembles is the energetics of the PDI chromophore. Ph-PDI has a higher energy of the singlet excited state, and it is a better electron acceptor. This makes the electron transfer feasible after excitation of either chromophore. Although we assume that the electron transfer takes place for the two other ensembles, as well, it can only start from the triplet state of the Ru(II) complex, which is higher in energy. Furthermore, ET takes place in the opposite direction, as compared with the ensemble 1,7(6)-Ph-PDI–Ru(II), and the CS states recombine quickly with time constants of 70 and 53 ps for 1,6-Py-PDI–Ru(II) and 1,7-Py-PDI–Ru(II), respectively. The electron-transfer rates and the obtained triplet-state lifetimes of the PDI moieties are summarized in Table 3.

**Table 3. Selected Photophysical Data of the PDI–Ru(II) Ensembles in Acetonitrile**

| compound | $\tau_T$[a] ($\mu$s) | $\tau_{CS}$[b] (ps) |
|---|---|---|
| 1,7-Py-PDI–Ru(II) | 57 | 3 |
| 1,6-Py-PDI–Ru(II) | 35 | 7 |
| 1,7(6)-Ph-PDI–Ru(II) | 62 | 86 |

[a]Triplet-state lifetime of the PDI moiety measured by nanosecond flash photolysis. [b]Rate of electron transfer, after excitation of the Ru(II) complex, obtained from pump–probe measurements.

## CONCLUSIONS

A series of metallo-organic PDI–$[Ru(bpy)_2dppz]^{2+}$ ensembles, consisting of either red or green PDI covalently linked to the Ru(II) polypyridine complex, have been synthesized and studied. In all the ensembles, strongly quenched emission of the PDI chromophore has been observed at all the excitation wavelengths. In addition, independent of the excited chromophore, the long-lived PDI-based triplet state was observed as the lowest excited state in the nanosecond transient absorption measurements. The transient absorption studies indicated that if the Ru(II) complex is excited, the conversion to the PDI triplet state takes place via a charge-transfer state, which has a higher energy than that of the triplet state. However, the direction of the electron transfer depends on the type of the PDI chromophore. For the ensemble 1,7(6)-Ph-PDI–Ru(II), the electron transfer is observed from Ru(II) to PDI, whereas for the other two ensembles, from PDI to Ru(II). When the PDI chromophore is excited, the electron transfer is observed only for the ensemble 1,7(6)-Ph-PDI–Ru(II). In the other two ensembles, the intersystem crossing is strongly facilitated, which is attributed to the presence of Ru in close vicinity to the excited PDI chromophore.

## EXPERIMENTAL SECTION

**Materials.** All the reagents utilized in the synthesis were purchased from Sigma-Aldrich, Co., and used as received unless otherwise stated. *N,N′*-Dioctyl-1,7(6)-dibromoperylene diimide **3** was synthesized according to the previously described procedure.[9,18] The solvents were of HPLC grade and purchased from VWR. Unless otherwise noted, they were used without further purification. Toluene was dried over sodium, and benzonitrile was distilled over $P_2O_5$ under an argon atmosphere prior to use. Thin-layer chromatography (TLC) was done on aluminum sheets precoated with Silica 60 $F_{254}$. The purification and isolation of the products were performed by column chromatography (silica gel 60, mesh size 40–63 $\mu$m, and silica gel 100, mesh size 63–200 $\mu$m). The TLC plates and the sorbents for the column chromatography were purchased from Merck.

**Instrumentation and Characterization.** The NMR spectra were recorded with a Varian Mercury 300 MHz spectrometer in $CDCl_3$ at room temperature. All chemical shifts are quoted relative to tetramethylsilane, $Si(CH_3)_4$ ($\delta$ = 0.0 ppm); $\delta$ values are given in ppm and $J$ values in Hz. High-resolution mass spectra were measured with a Waters LCT Premier XE ESI-TOF benchtop mass spectrometer. To obtain accurate mass values, we simultaneously infused the solution of the reference compound (leucine enkephaline) with analyte, and we processed the experimental spectra according to the routine of accurate mass measurements (peak centering and lock-mass TOF correction). Differential pulse voltammetry was performed using a potentiostat (Iviumstat compactstat IEC 61326 Standard) controlled by a PC with the software Iviumsoft (Version 1.752) in a three-electrode single-compartment cell consisting of a platinum-in-glass as the working electrode, Ag/AgCl as the reference electrode, and a graphite rod as the counter electrode. During the measurements, the values of pulse height, pulse width, and step voltage were set to 20 mV, 20 ms, and 2.5 mV, respectively. Benzonitrile containing 0.1 M tetrabutylammonium tetrafluoroborate was used as the solvent. The measurements were done under continuous flow of nitrogen. A $Fc/Fc^+$ couple was used as an internal standard, which exhibited oxidation at +0.48 V. The measurements were carried out in both directions: toward the positive and negative potential. The reduction and oxidation potentials were calculated as an average of the two scans.

All the spectroscopic measurements were carried out at room temperature. The absorption spectra were recorded with a Shimadzu UV-2501PC spectrophotometer and the fluorescence spectra using a Fluorolog-3 (SPEX, Inc.) fluorimeter. The emission spectra were corrected using a correction function supplied by the manufacturer. Fluorescence quantum yields of the red PDIs were determined relative to fluorescein ($\Phi_f$ = 0.92 in 0.1 N NaOH aqueous solution) and of green PDIs relative to cresyl violet ($\Phi_f$ = 0.54 in methanol).[19] Optical densities at the excitation wavelengths were maintained at around 0.1 to avoid reabsorption.

The flash-photolysis method was used to study time-resolved absorption in nano- to microsecond time scale with 10 ns laser pulses. The instrument has been described in detail elsewhere.[20] The samples were deoxygenated by the continuous bubbling of nitrogen throughout the measurements starting from 30 min prior to the measurement. Optical density of the solutions at the excitation wavelength was maintained at ≈0.6, and the excitation power density was maintained at 1 mJ/cm$^2$. Pump–probe technique with a time resolution of


dx.doi.org/10.1021/ic400474b | Inorg. Chem. 2013, 52, 9761–9773

~150 fs was used to detect the fast processes taking place in picosecond time scale. The instrument and the data analysis procedure have been described in detail earlier.[21] Shortly, the beam at the laser fundamental frequency (~840 nm) is split into two. A part of the beam goes through either a second harmonic generator or an optical parametric amplifier forming the excitation (pump) pulses at 420 or 600 nm, respectively. The other part is passed through a water cuvette generating a white continuum for detecting (probe) the absorbance changes in a wide spectral region. The probe beam is further split into two: a signal beam and a reference beam, which are both focused on the sample cuvette. The pump beam is passed through a delay line with a moving right angle reflector, which is used to tune the optical path length of the pump pulse relative to the probe pulse and focused on the signal beam in the sample cuvette. Depending on the position of the moving mirror on the delay line, the pump pulse arrives at the sample at a certain time before the probe pulse, and the absorption of the sample at a known time after the excitation is measured. By scanning the moving mirror through the entire delay line, one can detect changes in absorption starting from before the excitation (at negative delay times) to the upper limit of 1.2 ns after excitation, which is due to the limited length of the delay line. The raw data obtained from the measurements consist of the differential transient spectra at different delay times. From this primary data, transient absorption decay curves at different wavelengths can be drawn. In the data analysis procedure, the decay curves are fitted globally to a sum of exponentials

$$\Delta A(\lambda, t) = \sum a_i(\lambda)\exp\left(-\frac{t}{\tau_i}\right) \quad (1)$$

where $a_i$ is the amplitude and $\tau_i$ is the lifetime of the components. The number of components needed for a reasonable fitting of the data should give the number of transient species in the reaction, and the rate constants of the reaction steps can be calculated from the corresponding lifetimes. The transient absorption results in Figures 6a, 8a, S4, S6a, and S7 are presented as decay component spectra, where the amplitudes of the components from the fitting are plotted at each wavelength. Figures 6b, 8b, and S6b present time-resolved spectra at selected delay times calculated from eq 1.

**Synthesis of 6-Hydroxy-dipyrido[*a*,*c*]phenazine (1).** A mixture of 1,10-phenanthroline-5,6-dione (200.0 mg, 0.95 mmol) and 2,3-diaminophenol (130.0 mg, 0.10 mmol) was taken in a 100 mL round-bottom flask, and subsequently, ethanol (50 mL) was added. The reaction mixture was heated to reflux for 4 h. After it was cooled to room temperature, the solvent was evaporated under reduced pressure. The solid residue was dissolved in chloroform and purified by column chromatography on silica 100 using a 100:1 chloroform/ethanol mixture as eluent to remove the unreacted starting materials and 25:1 chloroform/ethanol to obtain the desired product (255 mg, 90%). $^1$H NMR (300 MHz, $CDCl_3$, $Si(CH_3)_4$): $\delta$ = 9.62 (dd, $J$ = 1.8, 8.2 Hz, 1H), 9.53 (dd, $J$ = 1.8, 8.2 Hz, 1H), 9.29 (dd, $J$ = 0.8, 1.8 Hz, 1H), 9.27 (dd, $J$ = 0.7, 1.8 Hz, 1H), 8.04 (s, 1H), 7.88 (m, 2H), 7.80 (m, 2H), 7.37 (dd, $J$ = 1.8, 7.0 Hz, 1H). MS (ESI-TOF): $[M - H]^-$ calcd for $C_{18}H_{10}N_4O$, 297.0776; found, 297.0795.

**Synthesis of Reference Ru(II) Complex (2).** 6-Hydroxy-dipyrido[*a*,*c*]phenazine **1** (30.0 mg, 0.10 mmol) was dissolved in ethanol (24 mL). Subsequently, $[Ru(bpy)_2Cl_2]\cdot 2H_2O$ (73.0 mg, 0.15 mmol) was added. The reaction mixture was heated at reflux for 16 h under argon atmosphere. After being cooled to room temperature, the solvent was evaporated in vacuo to obtain a solid residue, which was chromatographed on neutral alumina. First, 25:1 chloroform/ethanol was used as eluent to remove unreacted starting materials and eventually 1:1 chloroform/ethanol to collect the product. The solid residue was dissolved in the minimum amount of ethanol, and an aqueous solution of $NH_4PF_6$ (200.0 mg in 10 mL of water) was added dropwise under stirring. The dark brown precipitate was filtered, washed with several portions of water, and dried to yield the required product **2** (52.1 mg, 52%). MS (ESI-TOF): $[M - PF_6]^+$ calcd for $C_{38}H_{26}N_8OF_6PRu$, 857.0925; found, 857.0842. Anal. Calcd for $C_{38}H_{26}F_{12}N_8OP_2Ru$: C, 45.56; H, 2.62; N, 11.19. Found: C, 45.48; H, 2.57; N, 11.23.

**Synthesis of *N,N′*-Dioctyl-1-bromo-7(6)-(dipyridophenazinoxy)perylene-3,4,9,10-tetracarboxy Diimide (4).** A mixture of 6-hydroxy-dipyrido[*a*,*c*]phenazine **1** (87.0 mg, 0.29 mmol), $K_2CO_3$ (80.4 mg, 0.58 mmol), and 18-crown-6 (308 mg, 1.16 mmol) in dry toluene (200 mL) was stirred for 30 min under argon, and subsequently, *N,N′*-dioctyl-dibromoperylene diimide **3** (150 mg, 0.19 mmol) was added. The reaction mixture was stirred for 3 h at 90 °C under argon atmosphere. After being cooled to room temperature, the solvent was removed by rotary evaporation. The precipitate was thoroughly washed with several portions of water and dried. The crude product was purified by column chromatography on silica 100 using chloroform as eluent to afford the product **4** (165 mg, 86%), which was found to be a regioisomeric mixture of 1,7- and 1,6-substituted perylene diimide in a ratio of 60:40 (according to $^1$H NMR analysis). $^1$H NMR (300 MHz, $CDCl_3$, $Si(CH_3)_4$): $\delta$ = 9.89 (d, $J$ = 8.3 Hz, 0.6H), 9.87 (d, $J$ = 8.3 Hz, 0.4H), 9.73 (d, $J$ = 8.3 Hz, 0.6H), 9.72 (d, $J$ = 8.3 Hz, 0.4H), 9.64 (m, 1H), 9.26 (dd, $J$ = 2.1, 4.6 Hz, 1H), 9.04 (m, 1.5H), 8.90 (s, 0.4H), 8.82 (d, $J$ = 8.2 Hz, 0.5H), 8.68 (d, $J$ = 8.2 Hz, 0.6H), 8.63 (d, $J$ = 8.3 Hz, 1H), 8.55 (dt, $J$ = 2.0, 8.2 Hz, 1H), 8.35 (dd, $J$ = 1.8, 8.8 Hz, 1H), 8.24 (d, $J$ = 3.1 Hz, 1H), 8.00 (m, 1H), 7.81 (m, 2H), 7.13 (dd, $J$ = 4.6, 8.5 Hz, 0.6H), 7.05 (dd, $J$ = 4.6, 8.0 Hz, 0.4H), 4.17 (m, 2H), 4.02 (m, 2H), 1.71 (br, 2H), 1.60 (br, 2H), 1.40−1.16 (m, 20H), 0.83 (m, 6H). MS (ESI-TOF): $[M + H]^+$ calcd for $C_{58}H_{49}N_6O_5Br$, 991.3022; found, 991.3163.

**Synthesis of *N,N′*-Dioctyl-1-pyrrolidinyl-7-(dipyridophenazinoxy)perylene-3,4,9,10-tetracarboxy Diimide (5) and *N,N′*-Dioctyl-1-pyrrolidinyl-6-(dipyridophenazinoxy)perylene-3,4,9,10-tetracarboxy Diimide (6).** *N,N′*-Dioctyl-1-bromo-7(6)-(dipyridophenazinoxy)perylene diimide **4** (51 mg, 0.05 mmol) was dissolved in chloroform (40 mL). Subsequently, pyrrolidine (15 mL) was added portionwise. The reaction mixture was stirred at 55 °C under argon atmosphere. After some time, the reaction mixture turned deep green in color. The progress of the reaction was monitored by TLC, and after 4 h, the reaction mixture was allowed to cool to room temperature. Solvents were removed by rotary evaporation, and the crude product was purified by column chromatography on silica 100 using chloroform as eluent to yield the product (38 mg, 75%) as a dark green solid. $^1$H NMR spectrum (300 MHz, $CDCl_3$) revealed the presence of 1,7- and 1,6-regioisomers in a ratio of 68:32. The two regioisomers were separated from each other by column chromatography on silica 100 using 1:1 chloroform/toluene as eluent. The 1,7-regioisomer came first and the 1,6-regioisomer later.

***N,N′*-Dioctyl-1-pyrrolidinyl-7-(dipyridophenazinoxy)-perylene-3,4,9,10-tetracarboxy Diimide (5).** $^1$H NMR (300 MHz, $CDCl_3$, $Si(CH_3)_4$): $\delta$ = 9.92 (d, $J$ = 8.4 Hz, 1H), 9.61 (dd, $J$ = 1.8, 8.2 Hz, 1H), 9.25 (dd, $J$ = 1.8, 4.5 Hz, 1H), 9.03 (dd, $J$ = 1.8, 4.5 Hz, 1H), 8.86 (dd, $J$ = 1.8, 8.2 Hz, 1H), 8.63 (d, $J$ = 8.2 Hz, 1H), 8.59 (s, 1H), 8.35 (d, $J$ = 8.4 Hz, 1H), 8.29 (s, 1H), 8.24 (dd, $J$ = 1.3, 8.7 Hz, 1H), 7.91 (m, 1H), 7.80 (dd, $J$ = 4.4, 8.4 Hz, 1H), 7.68 (dd, $J$ = 1.2, 7.5 Hz, 1H), 7.61 (d, $J$ = 8.2 Hz, 1H), 7.12 (dd, $J$ = 4.4, 8.2 Hz, 1H), 4.17 (t, $J$ = 7.4 Hz, 2H), 4.05 (t, $J$ = 7.5 Hz, 2H), 3.80 (br, 2H), 2.83 (br, 2H), 2.20−1.96 (br, 4H), 1.78−1.54 (m, 4H), 1.44−1.14 (m, 20H), 0.83 (m, 6H). MS (ESI-TOF): $[M + Na]^+$ calcd for $C_{62}H_{57}N_7O_5Na$, 1003.4351; found, 1003.4304.

***N,N′*-Dioctyl-1-pyrrolidinyl-6-(dipyridophenazinoxy)-perylene-3,4,9,10-tetracarboxy Diimide (6).** $^1$H NMR (300 MHz, $CDCl_3$, $Si(CH_3)_4$): $\delta$ = 9.74 (d, $J$ = 8.5 Hz, 1H), 9.62 (dd, $J$ = 1.8, 8.0 Hz, 1H), 9.24 (dd, $J$ = 1.8, 4.6 Hz, 1H), 8.98 (dd, $J$ = 1.8, 4.5 Hz, 1H), 8.80 (d, $J$ = 8.1 Hz, 1H), 8.59 (d, $J$ = 8.4 Hz, 1H), 8.51 (s, 1H), 8.47 (dd, $J$ = 1.8, 8.1 Hz, 1H), 8.28 (dd, $J$ = 1.2, 8.7 Hz, 1H), 8.04 (s, 1H), 7.95 (m, 1H), 7.78 (m, 2H), 7.70 (d, $J$ = 8.2 Hz, 1H), 6.90 (dd, $J$ = 4.5, 8.2 Hz, 1H), 4.18 (t, $J$ = 7.7 Hz, 2H), 4.04 (t, $J$ = 7.5 Hz, 2H), 3.85 (br, 2H), 2.87 (br, 2H), 2.24−1.96 (br, 4H), 1.78−1.58 (m, 4H), 1.40−1.16 (m, 20H), 0.82 (m, 6H). MS (ESI-TOF): $[M + Na]^+$ calcd for $C_{62}H_{57}N_7O_5Na$, 1003.4351; found, 1003.4229.

**Synthesis of 1,7-Py-Perylene Diimide−Ru(II) Polypyridine Ensemble (1,7-Py-PDI−Ru(II), 7).** *N,N′*-Dioctyl-1-pyrrolidinyl-7-(dipyridophenazinoxy)perylene-3,4,9,10-tetracarboxy diimide **5** (6.8 mg,


dx.doi.org/10.1021/ic400474b | Inorg. Chem. 2013, 52, 9761−9773

0.007 mmol) was dissolved in DMF (5 mL), and subsequently, $[Ru(bpy)_2Cl_2]\cdot 2H_2O$ (6.7 mg, 0.014 mmol) was added. The reaction mixture was stirred at 110 °C for 18 h under argon atmosphere. Removal of the solvent by rotary evaporation gave a solid residue, which was chromatographed on neutral alumina. First 25:1 chlorofom/ethanol was used as eluent to remove unreacted starting materials and eventually 1:1 chloroform/ethanol to collect the desired product. The solid residue was dissolved in a minimum amount of ethanol, and an aqueous solution of $NH_4PF_6$ (97.0 mg in 5 mL water) was added dropwise under stirring. The green precipitate was filtered, washed with several portions of water, and dried to yield the required product (5.6 mg, 48%). MS (ESI-TOF): $[M - 2PF_6]^{2+}$ calcd for $C_{82}H_{73}N_{11}O_5Ru$, 696.7432; found, 696.7433. $[M - PF_6]^+$ calcd for $C_{82}H_{73}N_{11}O_5RuPF_6$, 1538.4504; found, 1538.4487. Anal. Calcd for $C_{82}H_{73}F_{12}N_{11}O_5P_2Ru$: C, 58.50; H, 4.37; N, 9.15. Found: C, 58.35; H, 4.33; N, 9.18.

**Synthesis of 1,6-Py-Perylene Diimide−Ru(II) Polypyridine Ensemble (1,6-Py-PDI−Ru(II), 8).** The title compound was prepared from *N,N′*-dioctyl-1-pyrrolidinyl-6-(dipyridophenazinoxy)perylene-3,4,9,10-tetracarboxy diimide **6** (5.1 mg, 5.2 μmol), $[Ru(bpy)_2Cl_2].2H_2O$ (5.0 mg, 10.4 μmol), and DMF (8 mL) following the procedure described above for the ensemble to obtain the product (4.3 mg, 49%). MS (ESI-TOF): $[M - 2PF_6]^{2+}$ calcd for $C_{82}H_{73}N_{11}O_5Ru$, 696.7432; found, 696.7393. $[M - PF_6]^+$ calcd for $C_{82}H_{73}N_{11}O_5RuPF_6$, 1538.4504; found, 1538.4502. Anal. Calcd for $C_{82}H_{73}F_{12}N_{11}O_5P_2Ru$: C, 58.50; H, 4.37; N, 9.15. Found: C, 58.62; H, 4.29; N, 9.11.

**Synthesis of *N,N′*-Dioctyl-1-pyrrolidinyl-7-(2,4-di-*tert*-butylphenoxy)perylene-3,4,9,10-tetracarboxy Diimide (9).** Compound **9** was synthesized in the following two steps. (i) First, *N,N′*-dioctyl-1-bromo-7(6)-(2,4-di-*tert*-butylphenoxy)perylene diimide was prepared from 2,4-di-*tert*-butylphenol (72.2 mg, 0.35 mmol), $K_2CO_3$ (97.0 mg, 0.70 mmol), 18-crown-6 (370 mg, 1.40 mmol), and *N,N′*-dioctyl-1,7(6)-dibromoperylene diimide **3** (180 mg, 0.23 mmol) in dry toluene (80 mL) according to the procedure described above for compound **4**. The crude product was chromatographed on silica 60 using toluene as eluent to afford the desired product (105 mg, 51%), which was a mixture of 1,7- and 1,6-regioisomers. $^1$H NMR (300 MHz, $CDCl_3$, $Si(CH_3)_4$): $\delta$ = 9.60 (d, $J$ = 8.2 Hz, 0.8H), 9.56 (d, $J$ = 8.2 Hz, 0.2H), 9.43 (m, 1H), 8.94 (s, 0.8H), 8.88 (s, 0.2H), 8.72 (d, $J$ = 8.2 Hz, 0.2H), 8.62 (m, 1.8H), 8.26 (s, 0.8H), 8.24 (s, 0.2H), 7.57 (d, $J$ = 2.4 Hz, 1H), 7.25 (dd, $J$ = 2.4, 8.5 Hz, 1H), 6.86 (d, $J$ = 8.5 Hz, 1H), 4.16 (m, 4H), 1.72 (m, 4H), 1.50−1.16 (m, 38H), 0.93 (m, 6H). MS (ESI-TOF): $[M + H]^+$ calcd for $C_{54}H_{61}N_2O_5Br$, 899.3836; found, 899.4002.

(ii) In the second step, a mixture of *N,N′*-dioctyl-1-bromo-7(6)-(2,4-di-*tert*-butylphenoxy)perylene-3,4,9,10-tetracarboxy diimide (80 mg, 0.09 mmol) and pyrrolidine (6 mL) was stirred under argon atmosphere for 14 h at 50 °C. After being cooled to room temperature, the reaction mixture was poured in 10% HCl (15 mL) under stirring and extracted with DCM (3 × 15 mL). The organic phase was dried over sodium sulfate, evaporated, and chromatographed (silica 100/toluene) to yield a green solid regioisomeric mixture (68 mg, 85%). The pure 1,7-regioisomer **9** was then separated from the mixture by column chromatography on silica 100 using toluene as eluent. $^1$H NMR (300 MHz, $CDCl_3$, $Si(CH_3)_4$): $\delta$ = 9.40 (d, $J$ = 8.5 Hz, 1H), 8.60 (d, $J$ = 8.1 Hz, 1H), 8.54 (s, 1H), 8.37 (d, $J$ = 8.5 Hz, 1H), 8.26 (s, 1H), 7.63 (d, $J$ = 8.1 Hz, 1H), 7.56 (d, $J$ = 2.4 Hz, 1H), 7.24 (dd, $J$ = 2.4, 8.5 Hz, 1H), 6.90 (d, $J$ = 8.5 Hz, 1H), 4.17 (m, 4H), 3.77 (br, 2H), 3.24 (br, 1H), 2.40 (br, 1H), 2.11 (br, 4H), 1.74 (m, 4H), 1.47 (s, 9H), 1.44−1.17 (m, 29H), 0.89 (m, 6H). MS (ESI-TOF): $[M]^+$ calcd for $C_{58}H_{69}N_3O_5$, 887.5237; found, 887.5290.

**Synthesis of *N,N′*-Dioctyl-1-(4-*tert*-butylphenoxy)-7(6)-(dipyridophenazinoxy)perylene-3,4,9,10-tetracarboxy Diimide (10).** The title compound was prepared according to the procedure described above for compound **4** from 4-*tert*-butylphenol (21.2 mg, 0.14 mmol), $K_2CO_3$ (39.0 mg, 0.28 mmol), 18-crown-6 (150 mg, 0.57 mmol), and *N,N′*-dioctyl-1-bromo-7(6)-(dipyridophenazinoxy)-perylene diimide **4** (70 mg, 0.07 mmol) in dry toluene (200 mL). The crude product was chromatographed on silica 60 using $CHCl_3$ as eluent to afford the regioisomeric mixture of the desired product **10** (84 mg, 75%). $^1$H NMR (300 MHz, $CDCl_3$, $Si(CH_3)_4$): $\delta$ = 9.98 (d, $J$ = 8.5 Hz, 0.6H), 9.94 (d, $J$ = 8.5 Hz, 0.3H), 9.57 (d, $J$ = 8.5 Hz, 1.1H), 9.50 (d, $J$ = 8.2 Hz, 0.9H), 9.26 (m, 1.1H), 9.02 (m, 1H), 8.79 (d, $J$ = 7.9 Hz, 0.7H), 8.75−8.56 (m, 1H), 8.52 (d, $J$ = 8.5 Hz, 0.9H), 8.47 (d, $J$ = 8.5 Hz, 0.8H), 8.36 (s, 0.7H), 8.32 (s, 0.7H), 8.23 (s, 0.3H), 8.18 (s, 0.2H), 7.98−7.83 (m, 0.7H), 7.78 (m, 2H), 7.63 (d, $J$ = 7.3 Hz, 0.8H), 7.52 (m, 2H), 7.19 (m, 2.7H), 7.08 (m, 0.4H), 3.99 (m, 4H), 1.60 (br, 4H), 1.41 (s, 9H), 1.37−1.16 (m, 20H), 0.83 (m, 6H). MS (ESI-TOF): $[M]^+$ calcd for $C_{68}H_{62}N_6O_6$, 1058.4725; found, 1058.4743.

**Synthesis of 1,7(6)-Ph-Perylene Diimide−Ru(II) Polypyridine Ensemble (1,7(6)-Ph-PDI−Ru(II), 11).** *N,N′*-Dioctyl-1-(4-*tert*-butylphenoxy)-7(6)-(dipyridophenazinoxy)perylene diimide **10** (10.0 mg, 9.5 μmol) was dissolved in DMF (20 mL) by stirring the suspension for 15 min at 100 °C. Subsequently, $[Ru(bpy)_2Cl_2]\cdot 2H_2O$ (9.1 mg, 18.9 μmol) was added. After that, a similar procedure was followed, as described above for compounds **7** and **8** to attain the required product **11** (10.7 mg, 64%). MS (ESI-TOF): $[M - PF_6]^+$ calcd for $C_{88}H_{78}N_{10}O_6RuPF_6$, 1617.4816; found, 1617.4910. Anal. Calcd for $C_{88}H_{78}F_{12}N_{10}O_6P_2Ru$: C, 59.96; H, 4.46; N, 7.95. Found: C, 59.85; H, 4.50; N, 7.76.

## ■ ASSOCIATED CONTENT

### Ⓢ Supporting Information

$^1$H−$^1$H COSY spectrum of ligand **5** (ref-1,7-Py-PDI); steady state emission spectrum of the ensemble 1,7(6)-Ph-PDI−Ru(II) in acetonitrile accompanied with that of ref-1,7(6)-Ph-PDI; differential pulse voltammograms of the all the ensembles; picosecond transient absorption decay component spectra of the compounds ref-Ru(II) and ref-1,7(6)-Ph-PDI; nanosecond transient absorption decay time profiles of the ensembles 1,7(6)-Ph-PDI−Ru(II) and 1,7-Py-PDI−Ru(II); picosecond transient absorption decay component spectra of the ensemble 1,6-Py-PDI−Ru(II); picosecond transient absorption decay component spectra of the ensemble 1,7-Py-PDI−Ru(II) obtained with excitation at 600 nm; nanosecond transient absorption spectrum and decay time profiles of the ensemble 1,6-Py-PDI−Ru(II); $^1$H NMR spectra of all synthesized compounds. This material is available free of charge via the Internet at http://pubs.acs.org.

## ■ AUTHOR INFORMATION


### Corresponding Author

*E-mail: rajeev.dubey@tut.fi. Fax: +358 3 364 1392.


### Notes

The authors declare no competing financial interest.

## ■ ACKNOWLEDGMENTS


The authors sincerely thank Dr. Mika Niskanen and Ms. Tuuva Kastinen for their help in understanding the structures and energetics of the PDI−Ru(II) ensembles. The financial support from the Academy of Finland is also gratefully acknowledged.


## ■ REFERENCES


(1) (a) Gust, D.; Moore, T. A.; Moore, A. L. *Acc. Chem. Res.* **1993**, *26*, 198−205. (b) Imahori, H.; Sakata, Y. *Adv. Mater.* **1997**, *9*, 537−546. (c) Gust, D.; Moore, T. A.; Moore, A. L. *Acc. Chem. Res.* **2001**, *34*, 40−48. (d) Wasielewski, M. R. *Chem. Rev.* **1992**, *92*, 435−461. (e) Lemmetyinen, H.; Tkachenko, N. V.; Efimov, A.; Niemi, M. *Phys. Chem. Chem. Phys.* **2011**, *13*, 397−412.

(2) (a) Würthner, F. *Chem. Commun.* **2004**, 1564−1579. (b) Huang, C.; Barlow, S.; Marder, S. R. *J. Org. Chem.* **2011**, *76*, 2386−2407.

(3) (a) Wasielewski, M. R. *J. Org. Chem.* **2006**, *71*, 5051−5066. (b) Wasielewski, M. R. *Acc. Chem. Res.* **2009**, *42*, 1910−1921. (c) Rybtchinski, B.; Sinks, L. E.; Wasielewski, M. R. *J. Am. Chem. Soc.* **2004**, *126*, 12268. (d) Perez-Velasco, A.; Gorteau, V.; Matile, S. *Angew.*

*Chem., Int. Ed.* **2008**, *47*, 921. (e) Hippius, C.; Schlosser, F.; Vysotsky, M. O.; Böhmer, V.; Würthner, F. *J. Am. Chem. Soc.* **2006**, *128*, 3870. (f) Gunderson, V. L.; Krieg, E.; Vagnini, M. T.; Iron, M. A.; Rybtchinski, B.; Wasielewski, M. R. *J. Phys. Chem. B* **2011**, *115*, 7533. (g) You, C.-C.; Hippius, C.; Grüne, M.; Würthner, F. *Chem.—Eur. J.* **2006**, *12*, 7510−7519. (h) Tomizaki, K.; Loewe, R. S.; Kirmaier, C.; Schwartz, J. K.; Retsek, J. L.; Bocian, D. F.; Holten, D.; Lindsey, J. S. *J. Org. Chem.* **2002**, *67*, 6519−6534. (i) Berberich, M.; Krause, A.; Orlandi, M.; Scandola, F.; Würthner, F. *Angew. Chem., Int. Ed.* **2008**, *47*, 6616.

(4) (a) Lukas, A. S.; Zhao, Y.; Miller, S. E.; Wasielewski, M. R. *J. Phys. Chem. B* **2002**, *106*, 1299−1306. (b) Dubey, R. K.; Niemi, M.; Kaunisto, K.; Efimov, A.; Tkachenko, N. V.; Lemmetyinen, H. *Chem.—Eur. J.* **2013**, *19*, 6791−6806.

(5) (a) Rachford, A. A.; Goeb, S.; Castellano, F. N. *J. Am. Chem. Soc.* **2008**, *130*, 2766−2767. (b) Prusakova, V.; McCusker, C. E.; Castellano, F. N. *Inorg. Chem.* **2012**, *51*, 8589−8598.

(6) Weissman, H.; Shirman, E.; Ben-Moshe, T.; Cohen, R.; Leitus, G.; Shimon, L. J. W.; Rybtchinski, B. *Inorg. Chem.* **2007**, *46*, 4790−4792.

(7) (a) Würthner, F.; Sautter, A.; Schmid, D.; Weber, P. J. A. *Chem.—Eur. J.* **2001**, *7*, 894−902. (b) Dobrawa, R.; Lysetska, M.; Ballester, P.; Grüne, M.; Würthner, F. *Macromolecules* **2005**, *38*, 1315−1325. (c) Golubkov, G.; Weissman, H.; Shirman, E.; Wolf, S. G.; Pinkas, I.; Rybtchinski, B. *Angew. Chem., Int. Ed.* **2009**, *48*, 926−930. (d) Tuccitto, N.; Delfanti, I.; Torrisi, V.; Scandola, F.; Chiorboli, C.; Stepanenko, V.; Würthner, F.; Licciardello, A. *Phys. Chem. Chem. Phys.* **2009**, *11*, 4033−4038. (e) Costa, R. D.; Céspedes-Guirao, F. J.; Bolink, H. J.; Fernández-Lázaro, F.; Sastre-Santos, Á.; Ortí, E.; Gierschner, J. *J. Phys. Chem. C* **2009**, *113*, 19292.

(8) (a) Prodi, A.; Chiorboli, C.; Scandola, F.; Lengo, E.; Alessio, E.; Dobrawa, R.; Würthner, F. *J. Am. Chem. Soc.* **2005**, *127*, 1454−1462. (b) Rodriguez-Morgade, M. S.; Torres, T.; Atienza-Castellanos, C.; Guldi, D. M. *J. Am. Chem. Soc.* **2006**, *128*, 15145−15154.

(9) Dubey, R. K.; Efimov, A.; Lemmetyinen, H. *Chem. Mater.* **2011**, *23*, 778−788.

(10) Zhao, Y.; Wasielewski, M. R. *Tetrahedron Lett.* **1999**, *40*, 7047−7050.

(11) (a) Ahrens, M. J.; Tauber, M. J.; Wasielewski, M. R. *J. Org. Chem.* **2006**, *71*, 2107−2114. (b) Goretzki, G.; Davies, E. S.; Argent, S. P.; Alsindi, W. Z.; Blake, A. J.; Warren, J. E.; McMaster, J.; Champness, N. R. *J. Org. Chem.* **2008**, *73*, 8808−8814.

(12) Goze, C.; Leiggener, C.; Liu, S.; Sanguinet, L.; Levillain, E.; Hauser, A.; Decurtins, S. *ChemPhysChem* **2007**, *8*, 1504−1512.

(13) Gholamkhass, B.; Koike, K.; Negishi, N.; Hori, H.; Takeuchi, K. *Inorg. Chem.* **2001**, *40*, 756−765.

(14) (a) Ford, W. E.; Kamat, P. V. *J. Phys. Chem.* **1987**, *91*, 6373−6380. (b) Shibano, Y.; Umeyama, T.; Matano, Y.; Tkachenko, N. V.; Lemmetyinen, H.; Araki, Y.; Ito, O.; Imahori, H. *J. Phys. Chem. C* **2007**, *111*, 6133−6142.

(15) (a) Flamigni, L.; Encinas, S.; Barigelletti, F.; MacDonnell, F. M.; Kim, K.-J.; Puntoriero, F.; Campagna, S. *Chem. Commun.* **2000**, 1185−1186. (b) Chiorboli, C.; Rodgers, M. A. J.; Scandola, F. *J. Am. Chem. Soc.* **2003**, *125*, 483−491. (c) Sun, Y.; Liu, Y.; Turro, C. *J. Am. Chem. Soc.* **2010**, *132*, 5594−5595.

(16) (a) Bhasikuttan, A. C.; Suzuki, M.; Nakashima, S.; Okada, T. *J. Am. Chem. Soc.* **2002**, *124*, 8398−8405. (b) Cannizzo, A.; Mourik, F.; Gawelda, W.; Zgrablic, G.; Bressler, C.; Chergui, M. *Angew. Chem., Int. Ed.* **2006**, *45*, 3174−3176. (c) Bräm, O.; Messina, F.; El-Zohry, A. M; Cannizzo, A.; Chergui, M. *Chem. Phys.* **2012**, *393*, 51−57.

(17) Ford, W. E.; Hiratsuka, H.; Kamat, P. V. *J. Phys. Chem.* **1989**, *93*, 6692−6696.

(18) Würthner, F.; Stepanenko, V.; Chen, Z.; Saha-Möller, C. R.; Kocher, N.; Stalke, D. *J. Org. Chem.* **2004**, *69*, 7933−7939.

(19) (a) Kreller, D. I.; Kamat, P. V. *J. Phys. Chem.* **1991**, *95*, 4406−4410. (b) Chen, Z.; Baumeister, U.; Tschierske, C.; Würthner, F. *Chem.—Eur. J.* **2007**, *13*, 450−465.

(20) Niemi, M.; Tkachenko, N. V.; Efimov, A.; Lehtivuori, H.; Ohkubo, K.; Fukuzumi, S.; Lemmetyinen, H. *J. Phys. Chem. A* **2008**, *112*, 6884−6892.

(21) (a) Tkachenko, N. V.; Rantala, L.; Tauber, A. Y.; Helaja, J.; Hynninen, P. H.; Lemmetyinen, H. *J. Am. Chem. Soc.* **1999**, *121*, 9378−9387. (b) Vehmanen, V.; Tkachenko, N. V.; Imahori, H.; Fukuzumi, S.; Lemmetyinen, H. *Spectrochim. Acta, Part A* **2001**, *57*, 2229−2244.